

# Regio- and Stereoisomeric Control of the Aggregation of Zinc-chlorins Possessing Inverted Interactive Hydroxyl and Carbonyl Groups

Shiki Yagai,<sup>†</sup> Tomohiro Miyatake,<sup>†,‡</sup> and Hitoshi Tamiaki<sup>\*,†,§</sup>

Department of Bioscience and Biotechnology, Faculty of Science and Engineering,  
Ritsumeikan University, Kusatsu, Shiga 525-8577, Japan

tamiaki@se.ritsumei.ac.jp.

Received May 11, 2001

As models for a self-aggregative, naturally occurring magnesium-chlorin bacteriochlorophyll-*d* possessing 3<sup>1</sup>-secondary alcoholic hydroxyl and 13<sup>1</sup>-oxo groups, zinc-chlorins were synthesized with 3<sup>1</sup>-oxo and 13<sup>1</sup>-secondary (**1**) or tertiary hydroxyl groups (**2**). Compared to the monomers in a tetrahydrofuran solution, diastereomers 13<sup>1</sup>*R*-**1R** and 13<sup>1</sup>*S*-**1S** gave red-shifted absorption maxima (643 → 674 nm in **1R** and 708 nm in **1S**) in 1 v/v% CH<sub>2</sub>Cl<sub>2</sub>–hexane solution, indicating their self-aggregation. Therefore, the positioning of the two groups at 3<sup>1</sup>/13<sup>1</sup> or 13<sup>1</sup>/3<sup>1</sup> on the N21–N23 molecular (Q<sub>y</sub>) axis is not necessarily important for the self-aggregation. The <sup>1</sup>H NMR and CD spectroscopic studies showed that the 674 nm absorbing species of **1R** was characterized as a face-to-face “closed” dimer, while the 708 nm absorbing species of **1S** was a large oligomer constructed with aggregation of head-to-tail “open” dimers. This diastereomeric control over the aggregation of **1R** and **1S** is more pronounced than that observed in the regioisomerically 3<sup>1</sup>-secondary alcoholic *R/S*-diastereomers **3R** and **3S**. The difference is ascribable to the conformational fixation of the 13<sup>1</sup>-hydroxyl group of the exo five-membered ring in **1**. In contrast to self-aggregative 3<sup>1</sup>-tertiary alcoholic **4**, both 13<sup>1</sup>-epimers of 13<sup>1</sup>-tertiary alcoholic **2** were monomeric even in nonpolar organic media: the additional 13<sup>1</sup>-methyl group (**1** → **2**) drastically suppressed the self-aggregation due to the interference of the methyl group in intermolecular  $\pi$ – $\pi$  interaction.

## Introduction

The self-organization of biomolecules in living organisms now attracts much attention. Although the structural building blocks and their organization processes are highly complicated, resulting supramolecular complexes are controlled by sophisticated noncovalent interactions. Investigation of natural supramolecular systems by a chemical approach helps us to understand these systems and promotes the development of new artificial supramolecular systems.

Our interest is currently focused on the self-assembly of the chlorophyllous pigments in chlorosomes, the main light-harvesting complexes of green bacteria. Chlorosomes are small organelles bound to the inner surface of the cytoplasmic membrane.<sup>1</sup> In the photosynthetic light-harvesting apparatus of algae and higher plants, chlorophylls such as chlorophyll (Chl)s-*a* and *b* are noncovalently bound to polypeptides to form supramolecular pigment–protein complexes. In contrast, chlorosomes possess a unique light-harvesting apparatus: chlorosomal chlorophylls, bacteriochlorophyll (BChl)s-*c*, *d*, and *e* (Figure 1), self-assemble to construct large and highly ordered aggregates and accomplish efficient light-

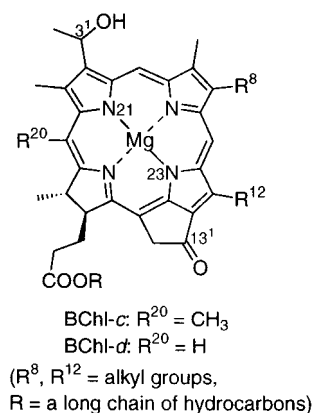


**Figure 1.** Main natural chlorophylls in extramembranous antenna complexes (chlorosomes) of green photosynthetic bacteria: molecular structures of chlorosomal chlorophylls.

harvesting and fast energy transfer processes without any protein scaffolds.<sup>2</sup> As a result, chlorosomes have received considerable attention due to this relatively simple supramolecular system. It is worth noting that the molecular structures of light-absorbing chlorophylls in the above two antenna systems are different in the following two points: BChls-*c*, *d*, and *e* possess a 1-hydroxyethyl group at the 3-position instead of the vinyl group of Chls-*a* and *b* and lack the 13<sup>2</sup>-methoxycarbonyl group that Chls-*a* and *b* have.

\* To whom correspondence should be addressed. Fax: +81-77-561-2659.

<sup>†</sup> Ritsumeikan University.

<sup>‡</sup> Current address: Department of Materials Chemistry, Faculty of Science and Technology, Ryukoku University, Otsu, Shiga 525-2194, Japan.

<sup>§</sup> “Form and Function” PRESTO, Japan Science and Technology Corporation (JST).

(1) Staehelin, L. A.; Golecki, J. R.; Drews, G. *Biochim. Biophys. Acta* **1980**, *589*, 30–45.

(2) (a) Holzwarth, A. R.; Griebenow, K.; Schaffner, K. *J. Photochem. Photobiol. A: Chem.* **1992**, *65*, 61–71. (b) Olson, J. M. *Photochem. Photobiol.* **1998**, *67*, 61–75.

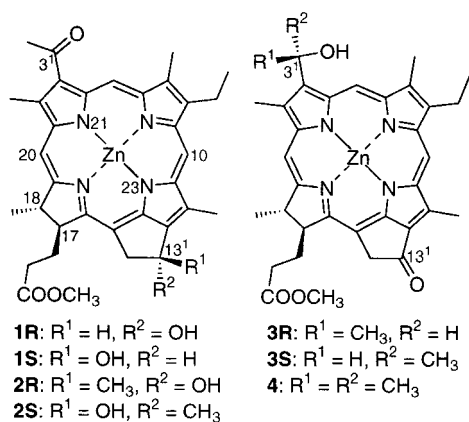


**Figure 2.** Synthetic zinc-3<sup>1</sup>-oxo-13<sup>1</sup>-hydroxy-chlorins **1** and **2** and zinc-3<sup>1</sup>-hydroxy-13<sup>1</sup>-oxo-chlorins **3** (zinc methyl bacteriopheophorbide-*d*) and **4**.

Since it was shown that BChl-*c* self-aggregates in a nonpolar organic solvent to form oligomers similar to those in native chlorosomes,<sup>3</sup> numerous model studies of chlorosomal chlorophyll aggregation have been reported using either intact magnesium-chlorophylls or their more stable zinc-chlorin analogues (for example, zinc-chlorin **3** in Figure 2) possessing 3<sup>1</sup>-hydroxyl and 13<sup>1</sup>-oxo groups.<sup>4,5</sup> These studies revealed that self-aggregation of chlorosomal chlorophylls was driven by intermolecular interaction among the 3<sup>1</sup>-hydroxyl, central metal, and 13-keto moieties, i.e.,  $C=O \cdots H-O \cdots Mg$  (or Zn) bonds, in addition to  $\pi$ - $\pi$  interaction between chlorin moieties. Several supramolecular structural models have been proposed for these pigment assemblies;<sup>5</sup> verification of the details has been proved to be elusive.

In contrast to Chls-*a* and *b*, which are bound to polypeptides to harvest sunlight and subsequently pass the excited energy to other molecules, the molecular structures of chlorosomal chlorophylls must be keyed to their self-assemblies, which are functional cores of the efficient light-harvesting and energy-transfer process of green bacteria. Indeed, chlorosomal chlorophylls are well designed to self-assemble efficiently. For example, the possession and the linear location of the three interactive sites (OH, Mg, C=O) on the Q<sub>y</sub> molecular axis (N21–N23 as in Figure 1) of the bacteriochlorophylls are vital for the construction of large, well-ordered aggregates that can function as efficient light-harvesting and energy-transfer materials.<sup>6,7</sup> The lack of the 13<sup>2</sup>-methoxycarbonyl group is also a prerequisite for close pigment–pigment contact.<sup>8</sup> Thus, examining the correlation between the molecular structure and the aggregation behavior of chlorosomal chlorophylls should provide future ideas in designing supramolecular self-assemblies.

Although the importance of the linear location of the three interactive sites for the self-aggregation has been reported, it had been unknown until recently whether the relative position of the hydroxyl and keto group on the Q<sub>y</sub> axis is important for the self-aggregation. Two preliminary reports investigating these positions have recently appeared. We have reported that zinc-3<sup>1</sup>-oxo-13<sup>1</sup>-*S*-hydroxy-chlorin **1S**, in which the 3<sup>1</sup>-hydroxyl and 13<sup>1</sup>-oxo groups of zinc methyl bacteriopheophorbide-*d* (**3**)<sup>4f,9</sup> were mutually exchanged, self-aggregated to form oligomers in 1 v/v% CH<sub>2</sub>Cl<sub>2</sub>–hexane.<sup>10</sup> Jesorka et al. have also showed that zinc-chlorins possessing 3-formyl and 13<sup>1</sup>-hydroxyl groups self-aggregate in 1 v/v% CH<sub>2</sub>Cl<sub>2</sub>–hexane.<sup>11</sup> These studies show that self-aggregation of chlorophyllous pigments is not disturbed by inverting the hydroxyl and carbonyl sites in the molecules.

In this paper, we report the syntheses of 13<sup>1</sup>-*S*-**1S** and its epimer 13<sup>1</sup>-*R*-**1R** and describe their self-aggregation behavior by visible, <sup>1</sup>H NMR, and CD spectroscopy and molecular modeling calculations. The aggregation mechanism of **1R** and **1S** is also discussed. We have already reported that zinc-chlorin **4** possessing tertiary alcoholic 3<sup>1</sup>-hydroxyl and 13<sup>1</sup>-oxo groups self-aggregates as does zinc-chlorin **3** possessing a secondary alcoholic 3<sup>1</sup>-hydroxyl group.<sup>12</sup> Therefore, we also herein report the synthesis of epimeric zinc-chlorins **2** possessing tertiary alcoholic 13<sup>1</sup>-hydroxyl and 3<sup>1</sup>-oxo groups and their situation in nonpolar organic solvents.

## Experimental Section

Visible absorption, CD, and fluorescence spectra were measured in air-saturated solvents at room temperature on a Hitachi U-3500 spectrophotometer, a Jasco J-720W spectropo-

(3) Bystrova, M. I.; Mal'gosheva, I. N.; Krasnovsky, A. A. *Mol. Biol.* **1979**, *13*, 440–451.

(4) (a) Smith, K. M.; Kehres, L. A.; Fajer, J. *J. Am. Chem. Soc.* **1983**, *105*, 1387–1389. (b) Brune, D. C.; Nozawa, T.; Blankenship, R. E. *Biochemistry* **1987**, *26*, 8644–8652. (c) Uehara, K.; Olson, J. M. *Photosynth. Res.* **1992**, *33*, 251–257. (d) Tamiaki, H.; Holzwarth, A. R.; Schaffner, K. *J. Photochem. Photobiol. B: Biol.* **1992**, *15*, 355–360. (e) Miller, M.; Gillbro, T.; Olson, J. M. *Photochem. Photobiol.* **1993**, *57*, 98–102. (f) Cheng, P.; Liddell, P. A.; Ma, S. X. C.; Blankenship, R. E. *Photochem. Photobiol.* **1993**, *58*, 290–295. (g) Hildebrandt, P.; Tamiaki, H.; Holzwarth, A. R.; Schaffner, K. *J. Phys. Chem.* **1994**, *98*, 2192–2197. (h) Wang, Z.-Y.; Umetsu, M.; Yoza, K.; Kobayashi, M.; Imai, M.; Matsushita, Y.; Niimura, N.; Nozawa, T. *Biochim. Biophys. Acta* **1997**, *1320*, 73–82. (i) Miyatake, T.; Tamiaki, H.; Holzwarth, A. R.; Schaffner, K. *Photochem. Photobiol.* **1999**, *69*, 448–456. (j) Ishii, T.; Uehara, K.; Ozaki, Y.; Mimuro, M. *Photochem. Photobiol.* **1999**, *70*, 760–765. (k) Miyatake, T.; Tamiaki, H. *Helv. Chim. Acta* **1999**, *82*, 797–810. (l) Mizoguchi, T.; Hara, K.; Nagae, H.; Koyama, Y. *Photochem. Photobiol.* **2000**, *71*, 596–609. (m) Balaban, T. S.; Leitich, J.; Holzwarth, A. R.; Schaffner, K. *J. Phys. Chem. B* **2000**, *104*, 1362–1372. (n) Tamiaki, H.; Kubo, M.; Oba, T. *Tetrahedron* **2000**, *56*, 6245–6257. (o) Oba, T.; Tamiaki, H. *Supramol. Chem.* **2001**, *12*, 369–378. (p) Kureishi, Y.; Shiraishi, H.; Tamiaki, H. *J. Electroanal. Chem.* **2001**, *496*, 13–20. (q) Saga, Y.; Matsura, K.; Tamiaki, H. *Photochem. Photobiol.* **2001**, *74*, 72–80. (r) Miyatake, T.; Oba, T.; Tamiaki, H. *ChemBioChem* **2001**, *2*, 335–342.

(5) (a) Tamiaki, H. *Coord. Chem. Rev.* **1996**, *148*, 183–197 and references therein. (b) Chiefari, J.; Griebenow, K.; Griebenow, N.; Balaban, T. S.; Holzwarth, A. R.; Schaffner, K. *J. Phys. Chem.* **1995**, *99*, 1357–1365. (c) Balaban, T. S.; Holzwarth, A. R.; Schaffner, K.; Boender, G.-J.; de Groot, H. J. M. *Biochemistry* **1995**, *34*, 15259–15266. (d) Tamiaki, H.; Amakawa, M.; Shimono, Y.; Tanikaga, R.; Holzwarth, A. R.; Schaffner, K. *Photochem. Photobiol.* **1996**, *63*, 92–99. (e) Tamiaki, H.; Miyata, S.; Kureishi, Y.; Tanikaga, R. *Tetrahedron* **1996**, *51*, 12421–12432. (f) Mizoguchi, T.; Sakamoto, S.; Koyama, Y.; Ogura, K.; Inagaki, F. *Photochem. Photobiol.* **1998**, *67*, 239–248. (g) Amakawa, M.; Tamiaki, H. *Bioorg. Med. Chem.* **1999**, *7*, 1141–1144. (h) Steensgaard, D. B.; Wackerbarth, H.; Hildebrandt, P.; Holzwarth, A. R. *J. Phys. Chem. B* **2000**, *104*, 10379–10386. (i) Tamiaki, H.; Amakawa, M.; Holzwarth, A. R.; Schaffner, K. *Photosynth. Res.* In press.

(6) Oba, T.; Tamiaki, H. *Photochem. Photobiol.* **1998**, *67*, 295–303.

(7) Yagai, S.; Miyatake, T.; Tamiaki, H. *J. Photochem. Photobiol. B: Biol.* **1999**, *52*, 74–85.

(8) Oba, T.; Tamiaki, H. *Photosynth. Res.* **1999**, *61*, 23–31.

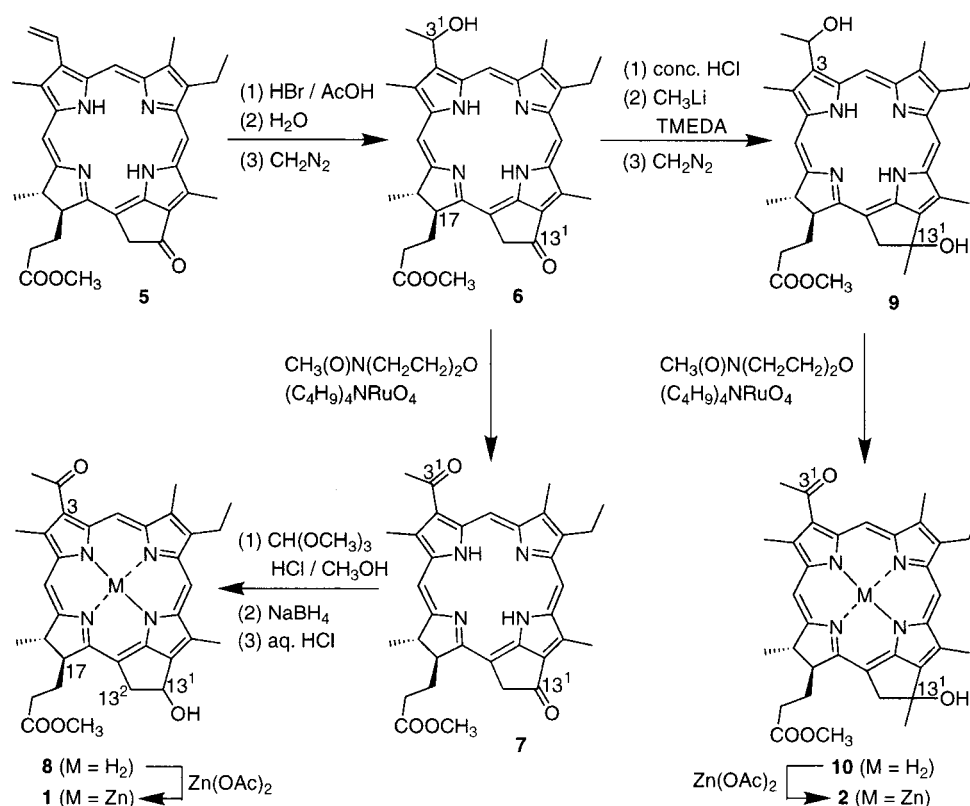
(9) (a) Tamiaki, H.; Takeuchi, S.; Tanikaga, R.; Balaban, T. S.; Holzwarth, A. R.; Schaffner, K. *Chem. Lett.* **1994**, 401–402. (b) Balaban, T. S.; Tamiaki, H.; Holzwarth, A. R.; Schaffner, K. *J. Phys. Chem. B* **1997**, *101*, 3424–3431. (c) Tamiaki, H.; Takeuchi, S.; Tsudzuki, S.; Miyatake, T.; Tanikaga, R. *Tetrahedron* **1998**, *54*, 6699–6718.

(10) Tamiaki, H.; Miyatake, T.; Tanikaga, R. *Tetrahedron Lett.* **1997**, *38*, 267–270.

(11) Jesorka, A.; Balaban, T. S.; Holzwarth, A. R.; Schaffner, K. *Angew. Chem., Int. Ed. Engl.* **1996**, *35*, 2861–2863.

(12) Yagai, S.; Miyatake, T.; Shimono, Y.; Tamiaki, H. *Photochem. Photobiol.* **2001**, *73*, 153–163.

Scheme 1



larimeter, and a Hitachi F-3500 fluorescence spectrophotometer, respectively. <sup>1</sup>H NMR measurements were performed on a Bruker AC-300 MHz NMR spectrometer. High-resolution (HR)- and fast atomic bombardment (FAB)-mass spectra (MS) were recorded on a JEOL HX-100 spectrometer; FAB-MS samples were dissolved in dichloromethane, and *m*-nitrobenzyl alcohol was used as the matrix. HPLC was carried out with a Shimadzu LC-10AS pump and a SPD-M10AV visible detector.

Hexane and dichloromethane for visible, CD, and fluorescence spectra were freshly distilled over CaH<sub>2</sub> before use. Methyllithium (MeLi, diethyl ether solution, 1.14 M) was purchased from Kanto Chemical Co. Flash column chromatography (FCC) was carried out on silica gel (Merck Kiesel gel 60, 9358). HPLC was performed with packed ODS columns (Cosmosil 5C18AR, Nacalai Tesque, 6.0 φ × 250 mm).

All synthetic zinc-chlorins and their intermediates were characterized by their visible, <sup>1</sup>H NMR, and FAB-MS spectra. Hydrolysis of the 17<sup>2</sup>-methoxycarbonyl group,<sup>13</sup> methylation of the keto group by MeLi and *N,N,N,N*-tetramethylethylenediamine (TMEDA),<sup>12</sup> oxidation of the secondary alcoholic 3<sup>1</sup>-hydroxyl group, and zinc metalation<sup>14</sup> were done according to reported procedures. Methyl 3-acetyl-3-devinyl-13<sup>1</sup>-deoxy-13<sup>1</sup>-hydroxy-pyropheophorbide-*a* (**8**) was prepared from **7** (Scheme 1).<sup>10,12</sup> Methyl bacteriopheophorbide-*d* (**6**)<sup>9c</sup> and methyl 3-acetyl-3-devinyl-pyropheophorbide-*a* (**7**)<sup>14</sup> were prepared by modification of methyl pyropheophorbide-*a* (**5**).<sup>5d</sup> All synthetic procedures were done in the dark. Molecular modeling calculations were performed according to reported procedures.<sup>12,15,16</sup>

**Synthesis of Zinc Methyl 3-Acetyl-3-devinyl-13<sup>1</sup>-deoxy-13<sup>1</sup>-hydroxy-pyropheophorbide-*a* (**1**).** Zinc metalation of 3-acetyl-3-devinyl-13<sup>1</sup>-deoxy-13<sup>1</sup>-hydroxy-pyropheophor-

bide-*a* (**8**) gave the titled compound **1** as a dark green solid in 91% yield. Each 13<sup>1</sup>-epimer **1R** and **1S** was separated by HPLC (**1R/1S** = 1.4/1, retention times were 9.2 min for **1R** and 11.2 min for **1S**; Cosmosil, MeOH/H<sub>2</sub>O = 9/1, 1.0 mL/min). **1R**: vis (THF) λ<sub>max</sub> 643 (rel intensity 35), 560 (5.0), 550 (2.0), 516 (4.0), 412 nm (100); <sup>1</sup>H NMR (10 v/v% CD<sub>3</sub>OD-CDCl<sub>3</sub>) δ 10.16, 9.51, 8.73 (each 1H, s, 5-, 10-, 20-H), 6.33 (1H, d, *J* = 6 Hz, 13-CH), 5.20 (1H, dd, *J* = 6, 16 Hz, 13<sup>1</sup>-CH anti to 13<sup>1</sup>-OH), 4.52–4.65 (1H, m, 18-H), 4.41 (1H, d, *J* = 16 Hz, 13<sup>1</sup>-CH syn to 13<sup>1</sup>-OH), 4.39 (1H, m, 17-H), 3.82 (2H, q, *J* = 7 Hz, 8-CH<sub>2</sub>), 3.64, 3.50, 3.46, 3.40, 3.24 (each 3H, s, 2-, 7-, 12-CH<sub>3</sub>, 3-COCH<sub>3</sub>, COOCH<sub>3</sub>), 2.45–2.72, 2.20–2.38, 2.00–2.17 (2H + 1H + 1H, m, 17-CH<sub>2</sub>-CH<sub>2</sub>), 1.81 (3H, d, *J* = 7 Hz, 18-CH<sub>3</sub>), 1.72 (3H, t, *J* = 7 Hz, 8<sup>1</sup>-CH<sub>3</sub>); HRMS (*m/z*) found 628.2028, calcd for C<sub>34</sub>H<sub>36</sub>N<sub>4</sub>O<sub>4</sub>Zn (M<sup>+</sup>) 628.2090. **1S**: vis (THF) λ<sub>max</sub> 643 (rel intensity 33), 601 (4.0), 554 (2.0) 516 (4.0), 412 nm (100); <sup>1</sup>H NMR (10 v/v% CD<sub>3</sub>OD-CD<sub>2</sub>Cl<sub>2</sub>) δ 10.09, 9.49, 8.73 (each 1H, s, 5-, 10-, 20-H), 6.301 (1H, d, *J* = 6 Hz, 13-CH), 5.10 (1H, dd, *J* = 6, 16 Hz, 13<sup>1</sup>-CH anti to 13<sup>1</sup>-OH), 4.52 (1H, dq, *J* = 2, 7 Hz, 18-H), 4.47 (1H, d, *J* = 16 Hz, 13<sup>1</sup>-CH syn to 13<sup>1</sup>-OH), 4.32 (1H, m, 17-H), 3.79 (2H, q, *J* = 7 Hz, 8-CH<sub>2</sub>), 3.59, 3.46, 3.37, 3.32, 3.17 (each 3H, s, 2-, 7-, 12-CH<sub>3</sub>, 3-COCH<sub>3</sub>, COOCH<sub>3</sub>), 2.60–2.72, 2.35–2.55, 2.10–2.30 (1H + 2H + 1H, m, 17-CH<sub>2</sub>-CH<sub>2</sub>), 1.74 (3H, d, *J* = 7 Hz, 18-CH<sub>3</sub>), 1.68 (3H, t, *J* = 7 Hz, 8<sup>1</sup>-CH<sub>3</sub>); HRMS (*m/z*) found 628.2074, calcd for C<sub>34</sub>H<sub>36</sub>N<sub>4</sub>O<sub>4</sub>Zn (M<sup>+</sup>) 628.2090.

**Synthesis of Zinc Methyl 3-Acetyl-3-devinyl-13<sup>1</sup>-deoxy-13<sup>1</sup>-hydroxy-13<sup>1</sup>-methylpyropheophorbide-*a* (**2**).** Hydrolysis of methyl bacteriopheophorbide-*d* (**6**, 30 mg; 3<sup>1</sup>-*R/S* = 1/1) gave the corresponding carboxylic acid as a brown solid after purification by recrystallization from CH<sub>2</sub>Cl<sub>2</sub>–hexane.

The 13-keto group of the above acid was methylated by MeLi (0.65 mL of 1.14 M diethyl ether solution) in the presence of TMEDA (0.5 mL) in dry THF (20 mL). Successive esterification by excess diazomethane in diethyl ether and purification by FCC (eluted with 1% MeOH–CH<sub>2</sub>Cl<sub>2</sub>) gave a 13<sup>1</sup>-epimeric mixture (1:2) of 3<sup>1</sup>,13<sup>1</sup>-dihydroxy-13<sup>1</sup>-methyl-chlorin **9** (22 mg) in 70% yield from **6**: vis (CH<sub>2</sub>Cl<sub>2</sub>) λ<sub>max</sub> 645 (rel intensity 26), 589 (10), 498 (10), 396 nm (100); <sup>1</sup>H NMR (CDCl<sub>3</sub>) δ (major/

(13) Miyatake, T.; Tamiaki, H.; Holzwarth, A. R.; Schaffner, K. *Photochem. Photobiol.* **1999**, *69*, 448–456.

(14) Tamiaki, H.; Yagai, S.; Miyatake, T. *Bioorg. Med. Chem.* **1998**, *6*, 2171–2178.

(15) Holzwarth, A. R.; Schaffner, K. *Photosynth. Res.* **1994**, *41*, 225–233.

(16) Kureishi, Y.; Tamiaki, H. *J. Porphyrins Phthalocyanines* **1998**, *2*, 159–169.



minor) 10.06/10.08, 9.65, 8.88 (each 1H, s, 5-, 10-, 20-H), 6.50–6.60 (1H, m, 3-CH), 5.05/5.12, 4.97/4.87 (each 1H, d,  $J = 16$  Hz, 13<sup>1</sup>-CH<sub>2</sub>), 4.58–4.60 (1H, m), 1.60 (1H, m, 18-H), 4.40–4.50 (1H, m, 17-H), 3.85 (2H, q,  $J = 8$  Hz, 8-CH<sub>2</sub>), 3.64, 3.54, 3.40/3.41, 3.37/3.38 (each 3H, s, 2-, 7-, 12-CH<sub>3</sub>, COOCH<sub>3</sub>), 2.45–2.89, 2.10–2.45 (each 2H, m, 17-CH<sub>2</sub>CH<sub>2</sub>), 2.31/2.40 (3H, s, 13<sup>1</sup>-CH<sub>3</sub>), 2.18 (3H, d,  $J = 7$  Hz, 3<sup>1</sup>-CH<sub>3</sub>), 1.86/1.87 (3H, d,  $J = 7$  Hz, 18-CH<sub>3</sub>), 1.76 (3H, d,  $J = 8$  Hz, 8<sup>1</sup>-CH<sub>3</sub>), –1.82, –3.37 (each 1H, s, NH); MS-FAB ( $m/z$ ) found 582, calcd for C<sub>35</sub>H<sub>42</sub>N<sub>4</sub>O<sub>4</sub> (M<sup>+</sup>) 582.

The above 3-(1-hydroxyethyl)-chlorin **9** was oxidized by catalytic tetrapropylammonium perruthenate and equivalent *N*-methylmorpholine and purified by FCC (eluted with 10–12% Et<sub>2</sub>O–CH<sub>2</sub>Cl<sub>2</sub>) to give 3-acetyl-chlorin **10** in 81% yield (13<sup>1</sup>-epimeric major/minor = 6/1); vis (CH<sub>2</sub>Cl<sub>2</sub>)  $\lambda_{\max}$  664 (rel intensity 29), 611 (4.0), 541 (4.0), 506 (11), 408 nm (100); <sup>1</sup>H NMR (CDCl<sub>3</sub>)  $\delta$  (major/minor) 10.4, 9.57, 8.99 (each 1H, s, 5-, 10-, 20-H), 5.11/5.07, 4.90/4.99 (each 1H, d,  $J = 16$  Hz, 13<sup>1</sup>-CH<sub>2</sub>), 4.57–4.70 (1H, m, 18-H), 4.40–4.50 (1H, m, 17-H), 3.85 (2H, q,  $J = 8$  Hz, 8-CH<sub>2</sub>), 3.76, 3.63, 3.41, 3.39/3.58, 3.36 (each 3H, s, 2-, 7-, 12-CH<sub>3</sub>, COCH<sub>3</sub>, COOCH<sub>3</sub>), 2.67–2.82, 2.50–2.65, 2.13–2.46 (1H + 1H + 2H, m, 17-CH<sub>2</sub>CH<sub>2</sub>), 2.32/2.41 (3H, s, 13<sup>1</sup>-CH<sub>3</sub>), 1.87/1.84 (3H, d,  $J = 7$  Hz, 18-CH<sub>3</sub>), 1.75 (3H, t,  $J = 8$  Hz, 8<sup>1</sup>-CH<sub>3</sub>), 0.07, –2.99 (1H, s, NH). HRMS ( $m/z$ ) found 581.3128, calcd for C<sub>35</sub>H<sub>38</sub>N<sub>4</sub>O<sub>4</sub> (M<sup>+</sup>) 581.3129.

Zinc metalation of **10** gave the titled compound **2** as a green solid in 92% yield. Epimers **2R** and **2S** were separated by HPLC (**2R/2S** = 1/3.2; retention times were 9.8 min for **2R** and 12 min for **2S**; Cosmosil, MeOH/H<sub>2</sub>O = 9/1, 1.0 mL/min). **2R**: vis (THF)  $\lambda_{\max}$  643 (rel intensity 34), 598 (4.5), 516 (4.0), 412 nm (100); <sup>1</sup>H NMR (CDCl<sub>3</sub>)  $\delta$  10.19, 9.61, 8.80 (each 1H, s, 5-, 10-, 20-H), 4.85 (2H, s, 13<sup>1</sup>-CH<sub>2</sub>), 4.55–4.63 (1H, m, 18-H), 4.33–4.47 (1H, m, 17-H), 3.86 (2H, q,  $J = 8$  Hz, 8-CH<sub>2</sub>), 3.58, 3.56, 3.39, 3.34, 3.22 (each 3H, s, 2-, 7-, 12-CH<sub>3</sub>, COCH<sub>3</sub>, COOCH<sub>3</sub>), 2.50–2.70, 2.25–2.50 (each 2H, m, 17-CH<sub>2</sub>CH<sub>2</sub>), 2.41 (3H, s, 13<sup>1</sup>-CH<sub>3</sub>), 1.85 (3H, d,  $J = 7$  Hz, 18-CH<sub>3</sub>), 1.75 (3H, t,  $J = 8$  Hz, 8<sup>1</sup>-CH<sub>3</sub>). HRMS ( $m/z$ ) found 642.2198, calcd for C<sub>35</sub>H<sub>38</sub>N<sub>4</sub>O<sub>4</sub><sup>64</sup>Zn (M<sup>+</sup>) 642.2185. **2S**: vis (THF)  $\lambda_{\max}$  643 (rel intensity 34), 598 (4.5), 515 (4.0), 412 nm (100); <sup>1</sup>H NMR (CDCl<sub>3</sub>)  $\delta$  10.03, 9.52, 8.77 (each 1H, s, 5-, 10-, 20-H), 4.86 (1H, d,  $J = 16$  Hz, 13<sup>1</sup>-CH anti to 13<sup>1</sup>-OH), 4.73 (1H, d,  $J = 16$  Hz, 13<sup>1</sup>-CH syn to 13<sup>1</sup>-OH), 4.51–4.62 (1H, m, 18-H), 4.30–4.41 (1H, m, 17-H), 3.80 (2H, q,  $J = 8$  Hz, 8-CH<sub>2</sub>), 3.60, 3.55, 3.36, 3.31, 3.15 (each 3H, s, 2-, 7-, 12-CH<sub>3</sub>, COCH<sub>3</sub>, COOCH<sub>3</sub>), 2.60–2.71, 2.38–2.60, 2.15–2.35 (1H + 2H + 1H, m, 17-CH<sub>2</sub>CH<sub>2</sub>), 2.27 (3H, s, 13<sup>1</sup>-CH<sub>3</sub>), 1.84 (3H, d,  $J = 7$  Hz, 18-CH<sub>3</sub>), 1.71 (3H, t,  $J = 8$  Hz, 8<sup>1</sup>-CH<sub>3</sub>). HRMS ( $m/z$ ) found 642.2146, calcd for C<sub>35</sub>H<sub>38</sub>N<sub>4</sub>O<sub>4</sub><sup>64</sup>Zn (M<sup>+</sup>) 642.2185.

## Results and Discussion

**Synthesis of Zinc-chlorins 1 and 2 Possessing 3<sup>1</sup>-Oxo and 13<sup>1</sup>-Hydroxyl Groups.** The preparation of 3-acetyl-13<sup>1</sup>-hydroxy-chlorin **8** (Scheme 1) was reported previously.<sup>10,12</sup> After dimethyl-ketal protection of the 3<sup>1</sup>-oxo group in 3<sup>1</sup>,13<sup>1</sup>-dioxo-chlorin **7**, the free 13<sup>1</sup>-oxo group was reduced by NaBH<sub>4</sub> to the 13<sup>1</sup>-hydroxyl group. Removal of the ketal-protecting group afforded chlorin **8** possessing inverted hydroxyl and keto groups compared to methyl bacteriopheophorbide-*d* (**6**). Insertion of zinc into **8** gave a diastereomeric mixture of zinc-chlorin **1** in 91% yield. The diastereomeric isomers of **1** were easily separated by a single HPLC run (Experimental Section), and their stereochemistries were determined by two-dimensional <sup>1</sup>H NMR techniques; in NOESY experiments, only **1S** showed evident <sup>1</sup>H–<sup>1</sup>H NOEs between 17-H ↔ 13<sup>2</sup>-H ↔ 13<sup>1</sup>-H. The ratio of 13<sup>1</sup>*R/S*-diastereomers was 1.4:1 (**1R/1S**) from the HPLC analysis, indicating that reduction of the 13<sup>1</sup>-oxo group was slightly stereoselective (17% diastereomeric excess (de)).

We previously reported that in the presence of TMEDA, MeLi smoothly reacted with keto and ester

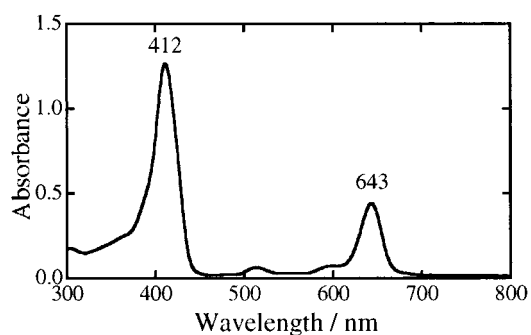


**Figure 3.** Visible absorption spectrum of **1R** (ca. 10  $\mu$ M) in neat THF.

groups of a chlorin to afford the tertiary alcohols.<sup>12</sup> To obtain tertiary alcoholic chlorin **2**, the reactive ester group of the 17-propionate in a 3<sup>1</sup>-epimeric mixture (**1**: **1**) of **6** was first deactivated by hydrolysis. The 13<sup>1</sup>-keto group of the resulting carboxylic acid was methylated selectively by MeLi and TMEDA (Scheme 1). After methylation of the carboxylic acid, a diastereomeric mixture of **9** possessing a tertiary alcoholic 13<sup>1</sup>-hydroxyl group was obtained in 70% yield from **6**. From the <sup>1</sup>H NMR spectra, the diastereomeric ratio for **9** at the 13<sup>1</sup>-position was 1:2, indicating that diastereospecific methylation occurred (ca. 30% de). The 3-(1-hydroxyethyl) group of **9** was oxidized to afford **10** in 81% yield. Finally, insertion of zinc into **10** gave the desired zinc-chlorin **2** possessing a tertiary alcoholic 13<sup>1</sup>-hydroxyl group and the 3<sup>1</sup>-oxo group (92% yield) as a diastereomeric mixture. The diastereomeric isomers of **2** were also easily separated by a single HPLC run (see Experimental Section), and their stereochemistries were determined in the same way as for **1** (2D <sup>1</sup>H NMR). From the HPLC analysis, the ratio of 13<sup>1</sup>*R/S*-diastereomers was 1:3.2 (**2R/2S**).

Epimerically pure **2R** and **2S** tended to readily epimerize by the inversion of the 13<sup>1</sup>-configuration at room temperature and transformed into a diastereomeric mixture, while **1R** and **1S** did not epimerize. This might be attributable to the stability of the tertiary carbocation at the 13<sup>1</sup>-position of **2** relative to the corresponding secondary carbocation of **1**. In the CDCl<sub>3</sub> solution, **2S** was the major product (86%) and **2R** was the minor product (14%) at equilibrium from the <sup>1</sup>H NMR analysis. Therefore, all spectroscopic experiments of diastereomerically pure **2R** and **2S** were performed immediately after the HPLC separation.

**Monomeric Zinc-chlorins 1 and 2 in THF.** Visible spectra of monomeric **1** and **2** solvated with tetrahydrofuran (THF) were measured in neat THF. The spectra of epimerically pure **1R**, **1S**, **2R**, and **2S** were almost identical (the spectrum of **1R** is shown in Figure 3) and had Soret and Q<sub>y</sub> maxima at approximately 412 and 643 nm, respectively. No visible spectroscopic differences were observed for each 13<sup>1</sup>-diastereomeric couple in the monomeric state. Furthermore, the similar visible spectra of **1** and **2** indicate that the additional 13<sup>1</sup>-methyl group did not affect the monomeric absorption properties. The Soret/Q<sub>y</sub> absorption ratios of **1** and **2** were approximately 3.1:1. The ratios in monomeric 3-acetyl-chlorins, which are larger than those in the corresponding 13<sup>1</sup>-oxo-chlorins (1.2–1.3:1),<sup>7</sup> were ascribed to the reduction of the 13-keto group strongly conjugated with the chlorin  $\pi$ -system.

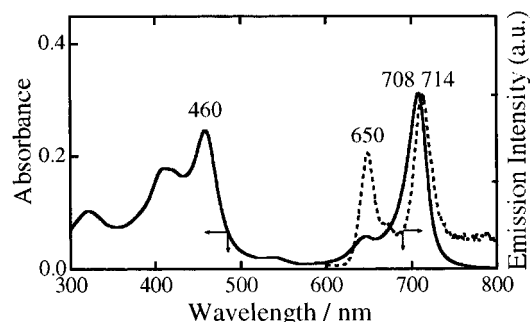


**Figure 4.** Visible absorption (solid curve) and fluorescence spectra (dashed curve, excited at 460 nm) of zinc-chlorin **1S** (ca. 10  $\mu$ M) in 1 v/v%  $\text{CH}_2\text{Cl}_2$ -hexane.

**Zinc-chlorin 1 in Nonpolar Media.** In 1 v/v%  $\text{CH}_2\text{Cl}_2$ -hexane, zinc-chlorin **1S** gave red-shifted absorption bands (solid curve in Figure 4) compared with those of the monomeric state. The new Soret and  $Q_y$  maxima of **1S** were 460 and 708 nm, respectively, red-shifted by 2530 and 1450  $\text{cm}^{-1}$  from those of monomers in THF, respectively. The Soret/ $Q_y$  absorption ratio drastically diminished to 0.8:1. Similar spectral changes induced by using less ligating solvents (from neat THF to 1 v/v%  $\text{CH}_2\text{Cl}_2$ -hexane) were observed in the *J*-aggregation of 3<sup>1</sup>-hydroxy-13<sup>1</sup>-oxo-type (natural-type) zinc-chlorins **3**<sup>4f,9</sup> and **4**<sup>12</sup> along the N21-N23 molecular ( $Q_y$ ) axis, indicating oligomerization of **1S** in nonpolar organic media. The fluorescence spectrum of the above nonpolar solution excited at 460 nm (dashed curve in Figure 4) showed a 714 nm emissive species in addition to a monomeric emission at 650 nm. This strongly indicates the presence of 708 nm absorbing aggregated species in the solution.

In contrast, zinc-chlorin **1R** in 1 v/v%  $\text{CH}_2\text{Cl}_2$ -hexane gave a broad red-shifted  $Q_y$  band that peaked at 674 nm immediately after preparation of the solution, and a monomeric band at 643 nm was also observed (Figure 5a). In comparison with the case of **1S**, a shoulder was observed on the longer wavelength region of the less red-shifted  $Q_y$  band. The second derivative (Figure 5b) of the visible spectra unambiguously showed a negative peak at 710 nm in addition to a major negative 674 nm peak. After preparation of the solution, the 710 and 643 nm bands gradually decreased concomitantly with an increase of the 674 nm band. Finally, the spectrum was changed to the solid curve in Figure 5c after standing for 1 h. By analogy with the 708 nm component of **1S**, the 710 nm absorbing component is speculated to be comprised of large aggregates, but the species was comprised of energetically unstable aggregates that changed into a more stable 674 nm species. Zinc-chlorin **1R** in nonpolar organic media attained the energetically stable aggregated state more slowly than did **1S**. The remaining monomer and large aggregates were confirmed by 643 and 710 nm minima in the second derivative of the  $Q_y$  absorption band (Figure 5d). Therefore, the resulting  $Q_y$  band consists of at least three components. The red-shift value of the major 674 nm absorbing component from the monomer at 643 nm is 715  $\text{cm}^{-1}$  and is considerably smaller than that of oligomeric **1S**. The 715  $\text{cm}^{-1}$  red-shift is reminiscent of small aggregated species such as a dimer, trimer, or tetramer.<sup>17</sup>

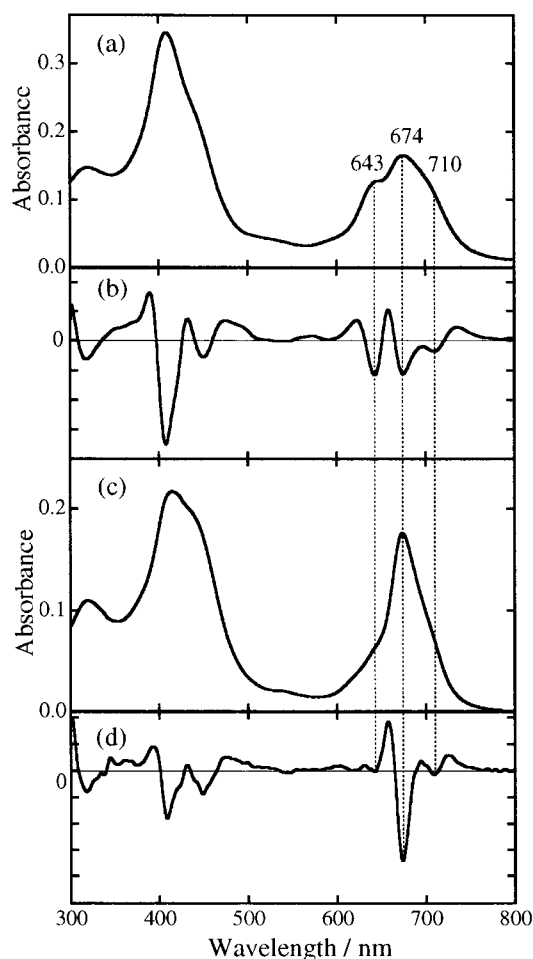


**Figure 5.** Visible absorption spectra of zinc-chlorin **1R** (ca. 10  $\mu$ M) in 1 v/v%  $\text{CH}_2\text{Cl}_2$ -hexane and their second derivatives: (a) visible spectrum immediately after preparation; (b) second derivative of visible spectrum (a); (c) visible spectrum after standing for 1 h; and (d) second derivative of visible spectrum (c).

The red-shift of absorption spectra is due to the strong excitonic coupling between closely interacting chromophores in the self-assembly.<sup>18</sup> Judging from the values of the red-shift of  $Q_y$  bands, 13<sup>1</sup>*S*-**1S** forms larger aggregates than 13<sup>1</sup>*R*-**1R** did. Time-dependent visible spectral changes of **1R** in the nonpolar media indicate that **1R** does not form large, energetically stable aggregates comparable to the 708 nm species of **1S**. The difference between the aggregation behavior of **1R** and **1S** is thus more clearly distinguishable than that of 3<sup>1</sup>-*R/S* diastereomers of zinc methyl bacteriopheophorbide-*d* (**3**).<sup>4f,9</sup> The conformational fixation of the interactive hydroxyl group at the 13<sup>1</sup>-position enhanced the diastereomeric control of the aggregation.

The visible absorption spectra in  $\text{CH}_2\text{Cl}_2$  solution of **1S** (4.6 mM) and  $\text{CHCl}_3$  solution of **1R** (ca. 3.5 mM) are shown in Figures 6a and 6b, respectively. Zinc-chlorin **1S** in concentrated  $\text{CH}_2\text{Cl}_2$  solution (Figure 6a) showed the 708 nm species coexisting with a larger amount of monomers than in diluted 1 v/v%  $\text{CH}_2\text{Cl}_2$ -hexane solution (Figure 4). The band shape of 708 nm species (Figure 6a) was almost identical to that formed in 1 v/v%  $\text{CH}_2\text{Cl}_2$ -hexane (Figure 4), indicating formation of the same

(17) Tamiaki, H.; Holzwarth, A. R.; Schaffner, K. *Photosynth. Res.* **1994**, *41*, 245-251.

(18) Buck, D. R.; Struve, W. S. *Photosynth. Res.* **1996**, *48*, 367-377.

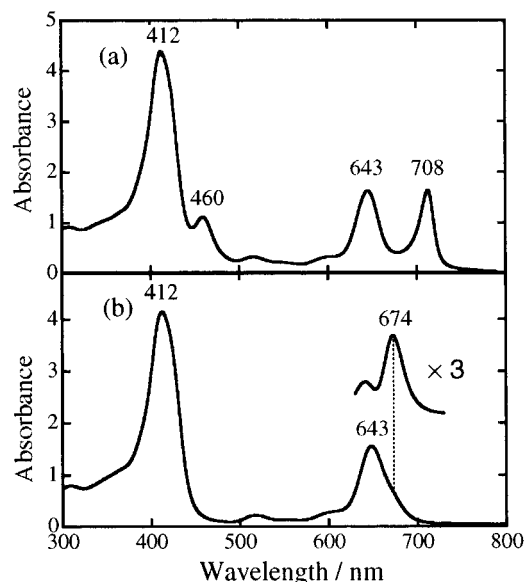
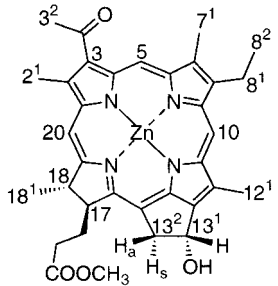


**Figure 6.** Visible spectra of zinc-chlorins: (a) concentrated  $\text{CH}_2\text{Cl}_2$  solution of **1S** (4.6 mM); (b) concentrated  $\text{CHCl}_3$  solution of **1R** (ca. 3.5 mM). Inset: difference spectrum at the  $Q_y$  region = (Figure 6b) –  $2.8 \times$  (Figure 3).

oligomer. In concentrated  $\text{CHCl}_3$  solution, **1R** showed a small shoulder at the red side of the monomeric  $Q_y$  absorption band (643 nm). Withdrawal of the monomeric spectrum presented in Figure 3 from the spectrum of Figure 6b gave the  $Q_y$  maxima at 674 nm (inset of Figure 6b), which is identical to that of the aggregate predominantly formed in 1 v/v%  $\text{CH}_2\text{Cl}_2$ –hexane (Figure 5c).

$^1\text{H}$  NMR spectra were measured in a concentrated  $\text{CDCl}_3$  solution of **1R** (ca. 3.5 mM) to investigate the 674 nm species formed in  $\text{CHCl}_3$  described above. Zinc-chlorin **1R** in neat  $\text{CDCl}_3$  showed that a clear  $^1\text{H}$  NMR spectrum differs from monomeric spectra (10 v/v%  $\text{CD}_3\text{OD}$ – $\text{CDCl}_3$ ). All resonances were averages of those in monomeric and aggregated states in the solution: no splitting of signals due to a rapid monomer  $\leftrightarrow$  aggregate equilibrium was observed. Because of this rapid equilibrium, no intermolecular correlation was observed in the ROESY spectra. The addition of  $\text{CD}_3\text{OD}$  induced shifts of these peaks by breaking up the aggregates to the monomer. The results are summarized in Table 1. The  $12^1$ -,  $13^1$ -, and  $13^2$ -protons around the  $13^1$ -hydroxyl group are strikingly high-field shifted in  $\text{CDCl}_3$  ( $\Delta\delta < -0.5$  ppm). This is attributed to the ring current effect of the adjacent interactive molecule,<sup>19</sup> indicating overlap of this region in the aggregated state and demonstrating the coordination of the hydroxyl group to the central zinc of the adjacent chlorin ( $\text{HO}\cdots\text{Zn}$ ). This was supported by the finding that the  $13^2$ -proton ( $\text{H}_s$ ) syn to the  $13^1$ -hydroxyl group was more shifted than the anti proton ( $\text{H}_a$ ). Other protons showed less changes in the chemical shifts ( $|\Delta\delta| < 0.2$  ppm). It should be noted that the protons ( $3^2\text{-H}_3$ ) of the 3-acetyl group did not show a large high-field shift comparable to protons around the  $13^1$ -hydroxyl group, indicating that the 3-acetyl group of **1R** was not involved in the aggregation. Given this, we propose a face-to-face closed dimer model in which each molecule mutually coordinates with the other as the aggregated structure

**Table 1.** Change of Chemical Shifts ( $\delta$ ) of Zinc-chlorin **1R** in  $\text{CDCl}_3$  with Addition of  $\text{CD}_3\text{OD}$



position	$\delta$ (aggregate)	$\delta$ (monomer) <sup>a</sup>	$\Delta\delta^b$
$2^1\text{-H}_3$	3.60	3.64	–0.04
$3^2\text{-H}_3$	3.11	3.24	–0.13
5-H	9.95	10.16	–0.21
$7^1\text{-H}_3$	3.30	3.40	–0.10
$8^1\text{-H}_2$	3.80	3.82	–0.02
$8^2\text{-H}_3$	1.76	1.72	0.04
10-H	9.36	9.51	–0.15
$12^1\text{-H}_3$	2.95	3.50	–0.55
$13^1\text{-H}$	5.50	6.33	–0.83
$13^2\text{-H}_s$	3.40	4.41	–1.01
$13^2\text{-H}_a$	4.60	5.20	–0.60
17-H	4.39	4.39	0.00
$\text{COOCH}_3$	3.43	3.46	–0.03
18-H	4.55	4.54	0.01
$18^1\text{-H}_3$	2.00	1.81	0.19
20-H	8.79	8.73	0.06

<sup>a</sup> In 10 v/v%  $\text{CD}_3\text{OD}$ – $\text{CDCl}_3$ . <sup>b</sup>  $\Delta\delta = \delta$  (aggregate) –  $\delta$  (monomer).

of the 674 nm species. The energy-minimized structure of such a dimer of **1R** by theoretical MM+/PM3 calculation is shown in Figure 7. This proposed structure is consistent with the observed high-field shifts of the  $12^1$ -,  $13^1$ -, and  $13^2$ -protons in  $\text{CDCl}_3$ .

In the above dimer, the  $Q_y$  ( $\text{N}21$ – $\text{N}23$ ) transition dipole moment of the upper molecule (solid arrow) was rotated counterclockwise by  $143^\circ$  to overlap the lower one (dashed arrow). When the chromophores excitonically couple in such a dimeric manner, negative chirality is expected from the exciton-chirality theory.<sup>20</sup> The CD spectrum of **1R** measured in 1 v/v%  $\text{CH}_2\text{Cl}_2$ –hexane (Figure 8) gave a reversed S-shape CD signal in the  $Q_y$  region, composed of a negative primary and a positive secondary Cotton effect, peaked at 702 and 674 nm, respectively, immediately after preparation of the solution. The solution that stood for 1 h showed a 1.5-fold larger intensity of both the CD signals. In light of the time-dependent increase of the 674 nm absorption in visible spectra of **1R** in 1 v/v%  $\text{CH}_2\text{Cl}_2$ –hexane (Figure 5), the CD spectra indicate that the reversed S-shape CD signal is derived from 674 nm absorbing species. On the basis that a reversed S-shaped CD signal indicates a negative chirality, the observed CD signal in the  $Q_y$  region supports the proposed face-to-face closed dimeric form (Figure 7) for the 674 nm absorbing species.

$^1\text{H}$  NMR measurements were performed for **1S** (4.5 mM) in concentrated  $\text{CD}_2\text{Cl}_2$  solution. The resulting spectrum only showed highly broadened monomeric resonances. This result implies that **1S** formed large colloidal aggregates and remained as a monomeric species in the solution (see Figure 6a), where the protons of the aggregate were significantly broad and could not be observed, and the protons of the residual monomer were

(19) Abraham, R. J.; Rowan, A. E.; Smith, N. W.; Smith, K. M. *J. Chem. Soc., Perkin Trans. 2* **1993**, 1047–1059.

(20) Harada, N.; Nakanishi, K. *J. Am. Chem. Soc.* **1969**, *91*, 3989–3991.



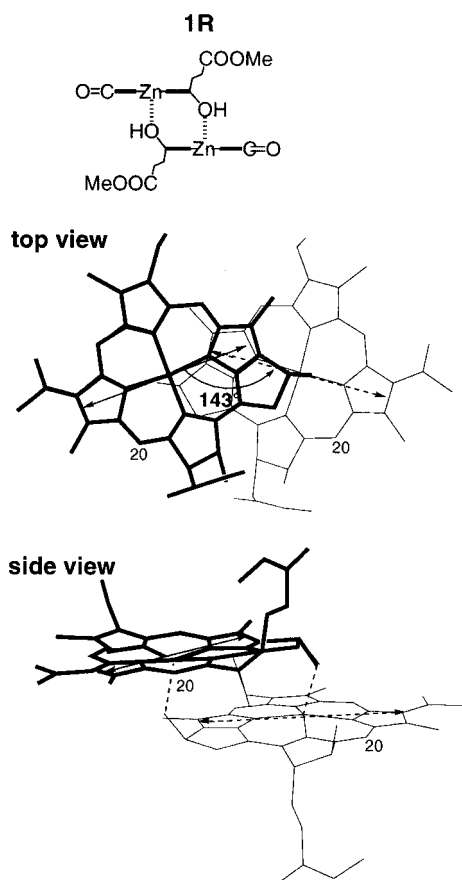


**Figure 7.** Energy-minimized face-to-face dimer of **1R**: (from top to bottom) schematic presentation, top view, and side view. For clarity, all hydrogens are omitted in these structures. Arrows indicate the  $Q_y$  transition dipole moments.

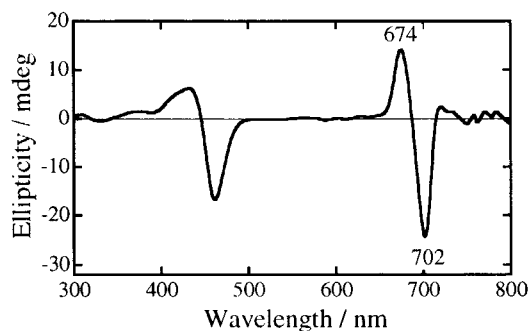


**Figure 8.** CD spectrum of **1R** (ca. 10  $\mu$ M) in 1 v/v%  $\text{CH}_2\text{Cl}_2$ –hexane immediately after preparation.

also broadened by the presence of the large aggregates.

Molecular modeling calculations were used to investigate the aggregation behavior of **1R** and **1S**. Three or two types of  $\pi$ – $\pi$  stacked structures in addition to monomers of **1R** and **1S** were modeled and energy-minimized by MM+ and/or PM3 calculations. The first is a parallel-type dodecamer<sup>12</sup> as shown in Figure 9: three head-to-tail tetramers formed by  $\text{H}-\text{O}\cdots\text{Zn}$  bonds are aligned in parallel by  $\text{C}=\text{O}\cdots\text{H}-\text{O}$  bonds. The parallel-type dodecamers would self-aggregate to give a large aggregate. The second is the face-to-face-type closed dimer (Figure 9) implied in the above  $^1\text{H}$  NMR and CD experiments. Only in **1R** is the third structure conceivable as a higher aggregate structure: an antiparallel-type dodecamer (Figure 9) based on dimeric units.<sup>5a</sup> In

this structure, closed dimers are linearly arranged by simultaneous formation of two hydrogen bonds between free oxygen atoms of 3-acetyl groups and hydrogen atoms of 13<sup>1</sup>-hydroxyl groups coordinated to zincs. Chains resulting from the association of closed dimers stack by  $\pi$ – $\pi$  interaction to make higher aggregates. The central zincs of the monomers and terminal chlorins in all the aggregate models were capped with 2-propanol to avoid any structural irregularity due to a lack of a fifth axial ligand. The modeled aggregation behavior is schematically shown in Figure 9, which should be referred to in the following discussion.

The stabilization energy of the parallel-type dodecamerization ( $\Delta E_{1-12} = (12E_1 - E_{12})/12$ ) of **1R** (path (i)) and **1S** (path (ii)) was 81 and 639 kJ/chlorin, respectively. This indicates that **1S** should form large aggregates (paths (ii) and (iv)) more readily than **1R** (paths (i) and (iii)). The stack-to-stack distance between adjacent columns of the tetramers was ca. 3.9 Å on average in dodecameric **1S** and 4.6 Å on average in dodecameric **1R**. The association of **1S** stacks, closer than that in **1R**, stabilizes the dodecamer by enhancement of  $\pi$ – $\pi$  interactions. On one hand, the 17-propionate groups of all molecules in dodecameric **1S** take the same conformation as in the corresponding monomeric form, indicating no interference of the 17-propionate groups with adjacent stacks. On the other hand, the 17-propionate groups of six molecules in dodecameric **1R** (surrounded by dashed lines in the parallel-type dodecamer of **1R** in Figure 9) are appreciably pressed down toward the plane of their own chlorins, indicating interference of 17-propionate groups with adjacent stacks. Groups of two 17<sup>1</sup>- and 17<sup>2</sup>-hydrogens are fairly close to a group of three hydrogens of the 3-acetyl group in the adjacent stack (2.5 and 2.6 Å apart, respectively). The 17-propionate groups in dodecameric **1R** obstruct close interaction between the stacks due to the steric repulsion of the 17- $\text{CH}_2\text{CH}_2$  moiety with the 3-acetyl group. When the acetyl group rotates around the  $\text{C}3-\text{C}3^1$  bond by 180° avoiding such an interatomic interference, formation of effective hydrogen bonds with the 13<sup>1</sup>-hydroxyl group is in turn sacrificed. Obviously, either situation of the 3-acetyl group could destabilize the dodecamer.

In contrast, the stabilization energy of face-to-face dimerization ( $\Delta E_{1-2} = (2E_1 - E_2)/2$ ) of **1R** (path (v)) and **1S** (path (vi)) in a “closed” manner was 416 and –67 kJ/chlorin, respectively. The large stabilization energy in **1R** strongly supports that **1R** predominantly forms a 674 nm species in 1 v/v%  $\text{CH}_2\text{Cl}_2$ –hexane as the face-to-face closed dimer (vide supra). Such a stable dimer can only grow into larger aggregates in a parallel manner by breaking the two  $\text{HO}\cdots\text{Zn}$  bonds followed by inversion of the chlorin plane in either dimeric molecule. Such molecular reorientation from face-to-face closed dimer to parallel type aggregates must involve a high energetic barrier and therefore is unlikely to occur in view of less stabilization of parallel type dodecamer ( $\Delta E_{1-12} = 81$  kJ/chlorin) relative to closed dimer ( $\Delta E_{1-2} = 416$  kJ/chlorin).

Another higher aggregate structure of **1R**, the antiparallel-type aggregate, remains controversial. As we have shown so far, the first step of antiparallel-type aggregation of **1R**, i.e., face-to-face closed dimerization, is undoubtedly possible. The stabilization energy of the trimerization from the closed dimer to the antiparallel hexamer ( $\Delta E_{2-6} = (3E_2 - E_6)/6$ ) was –419 kJ/chlorin (path (vii)). This energetically disadvantageous value is

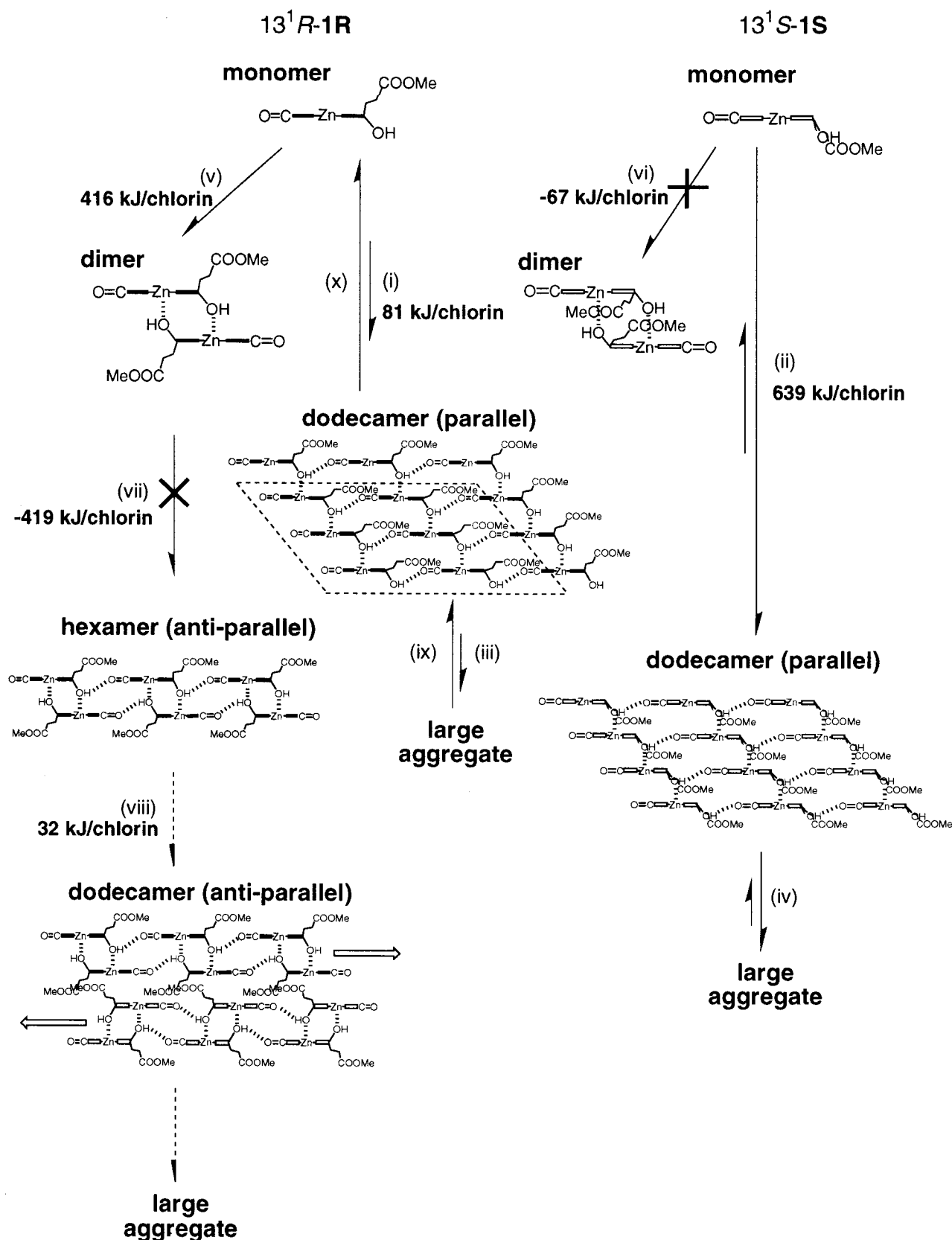


**Figure 9.** Schematic presentation of aggregation behavior of zinc-chlorins **1R** and **1S**. The opened and closed sides indicate the C10 and C20 sides of the chlorin plane, respectively (see Figure 2). In the parallel-type dodecamer of **1R**, the six molecules of which 17-propionate groups are pressed down toward the plane of their own chlorins are surrounded by a dashed line. The open arrows in the antiparallel-type dodecamer of **1R** indicate that two hexameric chains are oriented in opposite directions of each other. In these drawings, the 2-propanol caps of the central zinc of monomers and terminal chlorins have been omitted for clarity.

attributed to the absence of effective  $\pi$ - $\pi$  interaction between closed dimers in the hexamer. The next ag-

gregation process is the dimerization of the hexamer to the dodecamer. A hexameric chain of antiparallel dimers



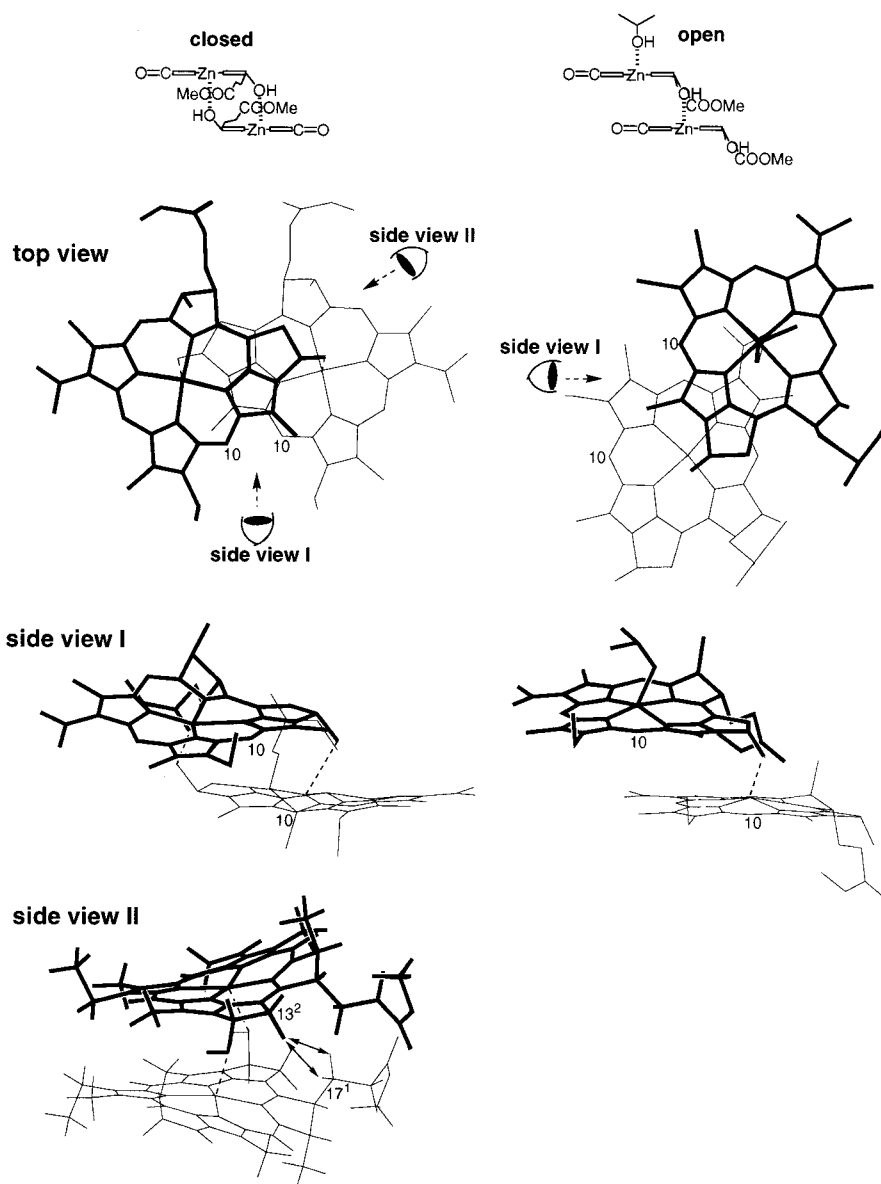


**Figure 10.** Energy-minimized face-to-face "closed" (left) and "open" dimers (right) of **1S**: (from top to bottom) schematic presentation, top view, side view I, and side view II. All hydrogens are omitted in these structures, except for side view II.

(Figure 7) has all the 17-propionate groups on one side of the chain (C20 side). These two chains could not stack enough to obtain effective  $\pi$ - $\pi$  interaction when oriented in the same direction because the 17-propionate groups of the second chain interact with those of first chain (Figure 9). Therefore, for the antiparallel-type higher aggregation of **1R**, two hexameric chains must stack in the manner in which the second chain is directed opposite to first chain as shown in Figure 9. The stabilization energy of the dimerization ( $\Delta E_{6-12} = (2E_6 - E_{12})/12$ ) from the hexamer to the dodecamer was 32 kJ/chlorin (path (viii)), indicating that effective  $\pi$ - $\pi$  interaction exists between two hexameric chains. Finally, the overall stabilization energy of the antiparallel dodecamerization from monomer to dodecamer ( $\Delta E_{1-12}$ ) was only 29 kJ/chlorin (paths (v) + (vii) + (viii)). In **1R**, antiparallel-type aggregation is less energetically favored than parallel-type aggregation ( $\Delta E_{1-12} = 81$  kJ/chlorin). This would be due to the high stability of closed dimer, which tends not to aggregate further. We concluded that antiparallel-

type aggregation to a higher aggregate via the closed dimer in **1R** does not occur.

Accordingly, the time-dependent visible spectral changes of **1R** in 1 v/v%  $\text{CH}_2\text{Cl}_2$ -hexane were explained as follows: (1) relatively unfavorable large aggregates (parallel type) are kinetically formed first (paths (i) and (iii)), (2) the aggregates are thermodynamically unstable relative to the closed dimer and broken into monomer (paths (ix) and (x)), and (3) the resulting monomers spontaneously dimerized to form the stable face-to-face dimer (path (v)).

In contrast, the negative  $\Delta E_{1-2}$  of **1S** indicates that the face-to-face dimer is not formed (path (vi)). The energy-minimized closed dimer of **1S** is shown in the left of Figure 10. The chlorin planes are considerably distorted compared with those of dimeric **1R** shown in Figure 7: standard deviations of 22 carbon and 4 nitrogen atoms of the chlorin skeleton with an exo five-membered ring from the mean plane were 0.30 Å for each molecule in dimeric **1S**, which is greater than the 0.10 Å

deviation in monomeric **1S** and the 0.13 Å deviation in dimeric **1R**. The 17-propionate group syn to the 13<sup>1</sup>-hydroxyl group in **1S** obstructs close face-to-face contact. The 13<sup>2</sup>-hydrogen syn to the 13<sup>1</sup>-hydroxyl group of one molecule interferes with the two 17<sup>1</sup>-hydrogens of the other molecule (2.2 and 2.3 Å apart, arrows of side view II in Figure 10). Therefore, **1S** favors an "open" dimeric form (the right of Figure 10) in which the 17-propionate group does not obstruct the molecular assembly. The open dimers self-assemble and grow into stable larger aggregates (paths (ii) and (iv)). Thus, the molecular modeling calculations predict very well the visible spectral observation of zinc-chlorin aggregation in 1 v/v% CH<sub>2</sub>Cl<sub>2</sub>-hexane.

**Zinc-chlorin 2 in Nonpolar Media.** In contrast to **1**, neither epimer of tertiary alcohol **2** showed obvious visible spectral changes in 1 v/v% CH<sub>2</sub>Cl<sub>2</sub>-hexane compared to those of the monomers in THF:  $\lambda_{\text{max}} = 412 \rightarrow 412$  nm (Soret) and  $643 \rightarrow 643$  nm ( $Q_y$ ); the Soret/ $Q_y$  absorption ratio = 2.9:1  $\rightarrow$  2.6:1 by neat THF  $\rightarrow$  1 v/v% CH<sub>2</sub>Cl<sub>2</sub>-hexane. The fluorescence spectra of the above solution excited at around 410–460 nm showed no emissive component other than a monomeric emission peaked at 652 nm. These results show that neither zinc-chlorin **2R** nor **2S** aggregated in 1 v/v% CH<sub>2</sub>Cl<sub>2</sub>-hexane. Aggregation of **2** could not be observed even in less polar organic solvents, e.g., 0.1 v/v% CH<sub>2</sub>Cl<sub>2</sub>-hexane. Therefore, the additional 13<sup>1</sup>-methyl group of **2** drastically disturbed the oligomerization. We previously reported that zinc-13<sup>1</sup>-oxo-chlorin **4** possessing a tertiary alcoholic 3<sup>1</sup>-hydroxyl group (zinc methyl 3<sup>1</sup>-methylbacteriopheophorbide-*d*) self-aggregated in 1 v/v% CH<sub>2</sub>Cl<sub>2</sub>-hexane to give red-shifted absorption bands ( $Q_y$  maximum at 704 nm) compared with the monomeric band.<sup>12</sup> It is worthwhile noting that the addition of a methyl group at the 3<sup>1</sup>- and 13<sup>1</sup>-positions affected self-aggregation differently, dependent upon the conformational flexibility of the neighboring hydroxyl group.

Model dodecamers of **2R** and **2S** were constructed in the same way as described above, and the supramolecular structures were energy-minimized by MM+/PM3 calculations. Compared with the parallel-type dodecameric energy-minimized structures of **1S** and **2S**, both the 13<sup>1</sup>-epimers showed Zn...OH coordinate bond lengths of approximately 1.9 Å, indicating that the additional 13<sup>1</sup>-methyl group does not affect the coordinate bond. The average angles of hydrogen bonding keto oxygen-hydroxyl hydrogen-hydroxyl oxygen (O...H-O) in dodecameric **1S** and **2S** are similar, 134 and 133°, respectively. However, the average distance between hydrogen bonding keto oxygen and hydroxyl hydrogen atoms (C=O...HO) in dodecameric **2S** was 3.1 Å, while that of **1S** was 2.5 Å. The former is considerably longer than the value in usual hydrogen bonding (~2.6 Å), indicating a weak hydrogen bond between the 3-C=O and 13<sup>1</sup>-OH groups in dodecameric **2S**. Furthermore, the stack-to-stack distance between adjacent tetrameric columns was ca. 4.6 Å on average in dodecameric **2S**, greater than the average of 3.9 Å in dodecameric **1S**. A large stack-to-stack distance means weak  $\pi$ - $\pi$  interaction. These factors lead to a smaller stabilization energy for the dodecamerization of **2S**: the  $\Delta E_{1-12}$  of **2S** was only 45 kJ/chlorin, while that of **1S** was 639 kJ/chlorin. The reason for the expanded stack-to-stack distance in dodecameric **2S** is the 13<sup>1</sup>-methyl group that projects into the  $\pi$ -plane of the neighboring chlorin; were the **2S** molecules to approach

each other as closely as **1S** molecules do, significant van der Waals repulsion would occur at several parts of the proposed dodecameric **2S**. The model study showed that oligomerization of **2S** via the parallel-type dodecamer is not favorable.

Similar modeling results were obtained for **1R** and **2R**. The hydrogen bond and the stack-to-stack distances of dodecameric **2R** (3.2 and 4.7 Å, respectively) were longer than those of dodecameric **1R** (2.5 and 4.3 Å, respectively), and **2R** showed a  $\Delta E_{1-12}$  of 54 kJ/chlorin, smaller than that of **1R** (81 kJ/chlorin). The model calculation predicts that **2R** should not form the parallel-type oligomers.

The face-to-face closed dimers of **2R** and **2S** were also modeled. Both energy-minimized structures were almost identical to those of **1R** and **1S**, respectively. The  $\Delta E_{1-2}$  values of **2R** and **2S** were 420 and -121 kJ/chlorin, respectively. The negative value in **2S** implies the impossibility of such a dimerization because of the same steric repulsion as in the case of **1S**, which is due to the 17-propionate group directed in the same way as the 13<sup>1</sup>-hydroxyl group. Therefore, **2S** should form neither a dimer nor an oligomer and remain monomeric even in the nonpolar media. The model study proposed that **2R** should form a closed face-to-face dimer similar to **1R**. Optical (visible, fluorescence, and CD) spectra of **2R**, even in neat hexane, showed the absence of such a dimer as well as any oligomers absorbing at >670 nm. Moreover, from the NMR spectrum in concentrated CDCl<sub>3</sub> solution (3.5 mM) at 0 °C, **2R** is seen to remain monomeric in the solution. Why **2R** does not dimerize is still an open question.

## Conclusion

Synthetic zinc-chlorin **1S** possessing 13<sup>1</sup>-hydroxyl and 3-keto groups aggregates to form oligomers similarly with the corresponding zinc-3<sup>1</sup>-hydroxyl-13-keto-chlorin **3**. The relative positions of the two interactive groups on the  $Q_y$  axis are unimportant for hydrogen and coordinate bonding, while the linear location of the three interactive sites including a central metal is necessary for the self-aggregation. In contrast, the 13<sup>1</sup>-epimeric **1R** predominantly associates to give an energetically stable face-to-face dimer. Transferring the 13-keto group to the 3-position and the 3<sup>1</sup>-hydroxyl group to the 13<sup>1</sup>-position in syn configuration to the 17-propionate group suppressed extended aggregation. In comparison with the natural-type metallochlorins possessing a more conformationally flexible 3-1-hydroxyethyl group as in **3**, 13<sup>1</sup>-diastereomeric control on the self-aggregation of **1R** and **1S** was more enhanced. The difference is ascribed to the conformational fixation of the interactive 13<sup>1</sup>-hydroxyl group as well as the fact that the 13<sup>1</sup>-stereocenter is closer to the inherent 17- and 18-stereocenters than the 3<sup>1</sup>-stereocenter is. Similar steric reasons explain that an additional 13<sup>1</sup>-methyl group as in **2** critically suppresses the self-aggregation.

**Acknowledgment.** We thank Drs. Tadashi Mizoguchi and Luke Ueda-Sarson of Ritsumeikan University for helpful discussions and Mrs. Yoshiyuki Shimono and Shuhei Hayakawa of the same institute for experimental assistance. S.Y. and T.M. thank the Japan Science Society for Sasakawa Scientific Research Grants.

**Supporting Information Available:** HPLC charts of zinc-chlorins **1** and **2**. This material is available free of charge via the Internet at <http://pubs.acs.org>.

JO010484X